Conjunctiva of Eye Color Change Assessment Using Microscope Image for Improving Tortuosity Through Empirical Wavelet Transform Compared with Neural Network - Forward

Krishna Kumari S[1] Dr.C.Murukesh[2]

[1]Department of ECE, Vel Tech High Tech Dr. Rangarajan Dr. Sakunthala Engineering College,
[2]Department of EEE, Velammal Engineering College

Abstract : The aim of this proposed work is to assess the eye color in conjunctiva using microscope images through Empirical Wavelet Transform (EWT) and compare it with the Neural Network Forward (NNF). Materials and Methods: The assessment was carried out for ten subjects whose eye images were captured using a microscope. Group 1 is considered as EWT, Group 2 is NNF, each consisting of ten samples totaling twenty samples. The number of samples was calculated with a pretest G power of 80 % and an error rate of 0.05. Results: The statistical analysis was done using SPSS, in EWT the average entropy was obtained was 3.5301 which is higher than obtained through NNF 2.9702. Conclusion: Eye color change assessment through novel EWT is significantly better than the NNF algorithm. Within the limitations of this study, tortuosity measurement using the eye through EWT has a higher significance than an NNF.

IndexTerms **- Conjunctiva, Eye Color Change Assessment, Empirical Wavelet Transform, Neural Network, Tortuosity, Feature extraction.**

I. INTRODUCTION

The conjunctiva is a thin membrane that covers the eye's surface and exposes the tiny blood vessels of the microcirculation for non-invasive assessment (Ganesh et al. 2017) . There are two types of the conjunctiva. They are bulbar conjunctiva, palpebral conjunctiva. The bulbar conjunctiva covers the anterior section of the sclera (the white of the eye). The bulbar conjunctiva terminates at the sclera-cornea junction and does not cover the cornea. The palpebral conjunctiva covers the inner surface of both the upper and lower eye libs (another term for the palpebral conjunctiva is tarsal conjunctiva (Iroshan et al. 2018). Signs of the conjunctiva are when small blood vessels in the conjunctiva become inflamed, they are more visible causing the sclera of our eyes to appear reddish or pink. Remedies, compresses and artificial tears, which are accessible without a prescription, can be used (Fielding 2008). Wear contact lenses just until your eye doctor advises it's safe to do so. Conjunctivitis does not generally result in persistent visual issues. However, if the symptoms are severe and not appropriately managed, it might cause harm in rare circumstances (Katzir and Martin 2008).

For the past 5 years, research going on for conjunctiva of eye color change assessment has resulted in around 29 articles in IEEE Xplore, 951 papers in Google scholar and 394 articles in ScienceDirect. Image of the anterior conjunctiva of the eye is captured using a Standard back-facing camera in a smartphone and it is applied for preprocessing. RGB spectrum was estimated to differentiate anemic and non-anemic patients. The accuracy is found to be 78.9 % (Tamir et al. 2017). Mice were killed through cervical dislocation, and the conjunctiva-containing eyeball was removed, fixed in 4% paraformaldehyde, and embedded in paraffin, eyeballs were sectioned in a vertical plane that was 4μm thick, the goblet cells were counted using an Olympus microscope (Chen et al. 2014). Their technique of research is to assess the tortuosity of the retinal microvasculature. They investigated if the tortuosity of the superior bulbar conjunctiva's macro vessels was connected to the existence of diabetes (Iroshan et al. 2018)**.** Their technique of research presents a method for extracting the PPG (Photoplethysmography) waveform from conjunctival videos with two motion-induced interferences.

Tortuosity diagnosis and management have not been studied previously, and tortuosity detection has been done using various techniques. Tortuosity Curvature Chain Code (TCCC) was previously used as a parameter to identify tortuosity. EWT is used in this work to identify changes in eye color by computing tortuosity values. The current DWT has the drawback of having poor tortuosity and efficiency. The purpose of the study is to find novel Conjunctiva of eye color change evaluation utilizing thermal images obtained by EWT and compared to DWT.

II. MATERIALS AND METHODS

This study is being conducted in the Department of Electronics and Communication Engineering at Saveetha School of Engineering. Two groups were taken, one group refers to EWT and the others refers to NNF technique. The required samples for this analysis are done using G power calculation. Preset power analysis was carried out at 80 %. Sample size of each group is 10 and the total sample size is 20 with a standard deviation for EWT = .03621 and NNF = .02011 using G power (Mc Cormick and Salcedo 2017).

In group 1, EWT is involved. The original image of an eye is captured through a thermal camera and thermal image is obtained and undergoes feature extraction through EWT and EWT2D filters are evolved and image is resynthesized and it is shown in fig. 2.

In group 2, DWT is involved. Here the original image of an eye is converted to a thermal image using a thermal camera and feature extraction is done through DWT and synthesized image is obtained and it is shown in fig. 3.

An image of a human eye is captured through a microscope. MATLAB 2021a software is used for further processing in HP Intel Core i5 5th generation CPU with 12GB of RAM. First, the image is recorded and it is converted to a grayscale image then

through EWT2D the image is aligned in order from left to right. After we see the partitioning of the fourier spectrum of the Littlewood paley testing. After that, minimizing and maximizing the value of the array is done to get outputs. We get Mean, Standard deviation and Entropy of an image as outputs. Once the process is finished, the tortuosity value will appear.

Simulation has been carried out in MATLAB. SPSS software is used to obtain graphs and tables. Analysis has been done by comparing two groups of EWT and Noninvasive measurement, each group having 10 test samples. For the above image processing technique, the system should support the 1TB HDD and 16GB RAM and intel i5 processor with 8th Generation.

III. EMPIRICAL WAVELET TRANSFORM

In compressive sensing, adaptive methods are used to evaluate a signal and detect sparse representations. For some source-processed signal designs, "rigid" methods such as wavelets or Fourier transforms are used. Adaptive methods build a basis based on the signal's data. The pursuit methods are used to create an adaptive representation in the wavelet packet transform. The wavelet transform produces interesting results in practical applications, and the wavelet packets are dependent on the specified subdivision scheme. Several approaches are used to create an adaptive representation, including the "Empirical Mode Decomposition" (EMD) algorithm.

IV. EMPIRICAL MODE DECOMPOSITION

The EMD's primary objective is to classify the main "modes." The signal modes are defined as follows: (roughly speaking, the mode is equivalent to the signal, comprising the Fourier transform). The EMD approach is capable of distinguishing the signal's non-stationary and stationary components. The lack of mathematical theory is the main disadvantage of the EMD system. In fact, the EMD method is an algorithmic method that is difficult to model due to its non-linearity. Nonetheless, some studies show that EMD functions similarly to an adaptive filter bank. Used an Amplitude Modulated-Frequency Modulated (AM-FM) signal to model a mode. The AM-FM signal properties are used to describe the entire signal in a function. The author is able to recover the different modes by minimizing this feature. To remove AM-FM signal components, use the EWT, which can create adaptive wavelets.

The EMD technique is a unique technique. The EMD is used to decompose a signal into its individual modes, and it was first proposed by(Huang et al. 1998). The EMD is a self-adapting method that corresponds to the signal $f(t)$ that has been analyzed, but it is not used in any permitted operation. The EMD assists in decomposing a signal $f(t)$as a finite sum of N+1 Intrinsic Mode Functions (IMF) $fk(t)$ using the Fourier formalism

$$f(t) = \sum_{k=0}^{N} f_k(t) \quad (1)$$

An Intrinsic Mode Functions (IMF) is an amplitude Modulated-frequency modulated function (AM-FM) which can be described as follows,

$$f_k(t) = F_k(t)cos(\varphi_k(t)) \quad (2)$$

Where , $F_k(t), \varphi_k'(t) > 0 \; \forall t$ (3)

The F_k and ψ'_k are slower than $\psi_{k.N}$ .The Intrinsic mode function f_k acts as a harmonic component. To extract intrinsic mode functions, the Huang method is used. The Huang method is a pure algorithmic method. For an intrinsic mode functions candidates are removed by calculating the lower, $\underline{f}(t)$and upper $\underline{f}(t)$, envelopes through a cubic spline interpolation from the minima and maxima off. By using m(t) = ($\underline{f}(t)$+ $\underline{f}(t)$)/2 , the mean envelope is obtained. Normally, $r_1(t)$ does not fulfill the intrinsic mode functions properties. By using the iteration process, the good candidate can be achieved to the subsequent r_k and $r_1$and. The last retained intrinsic mode function is f1(t) = rn(t). The EWT algorithm is highly adaptable and able to remove the non-stationary part of the real function. The real function is based on the ad-hoc process, mathematically difficult to model. The provided EMD signal is very difficult to understand. When the signals have noises, the problem can appear. So, the new approach Ensemble EMD (EEMD) is presented. The Ensemble EMD is used to calculate different EMD decompositions of the real signal. This real signal is corrupted by several artificial noises.

The Empirical Wavelets method is presented to create wavelets adapted to the processed signal. If the Fourier point of view is taken in the empirical wavelets, the group of wavelets adapted corresponds to total bandpass filters. The bandpass filter is used to reach adaptability, based on where the data is located in the analyzed signal spectrum. In fact, the Intrinsic Mode Functions properties correspond to the IMF spectrum centered around a specific frequency and compact support. For clarity purposes, I have to consider only real signals (the IMF spectrum is symmetric which corresponds to the frequency ω = 0), so it can be easily extended for the following reasoning to complex signals by creating several filters in Negative and Positive frequencies, respectively. Also, have to consider a normalized Fourier axis, which has a 2∏.

Let us assume that the Fourier support [0,π] is sectionalized into N contiguous segments .ω_n represents the limits between every segments also, each segment is represented as $\Delta_n = [\omega_{n-1}, \omega_n]$, then it is easy to prove $\cap_{n=1}^{N} \quad \wedge_n = [0, \pi]$.

The empirical wavelets represent bandpass filters on each $\wedge_n$. So, both Meyer's and Little wood-Paley wavelets used the empirical wavelets. Then $\forall_n > 0$, the empirical scaling function is expressed in equation (3) and empirical wavelets are expressed in (4) equation, respectively

$$\begin{aligned} \hat{\phi_n}(\omega) &= 1 && if\ |\omega| \le \omega_n - \tau_n \\ \hat{\phi_n}(\omega) &= cos\left[\frac{\pi}{2}\beta\left(\frac{1}{2\tau_n}(|\omega| - \omega_n + \tau_n)\right)\right] && if\ \omega_n - \tau_n \le |\omega| \le \omega_n + \tau_n \\ \hat{\phi_n}(\omega) &= 0 && otherwise \end{aligned} \quad (4)$$

$$\hat{\phi_n}(\omega) = 1\ if\ \omega_n + \tau_n \le |\omega| \le \omega_{n+1} - \tau_{n+1}$$

$$\hat{\psi_n}(\omega) = cos\left[\frac{\pi}{2}\beta\left(\frac{1}{2\tau_{n+1}}(|\omega| - \omega_{n+1} + \tau_{n+1})\right)\right]\ if\ \omega_{n+1} - \tau_{n+1} \le |\omega| \le \omega_{n+1} + \tau_{n+1}$$

$$\hat{\phi_n}(\omega) = \sin\left[\frac{\pi}{2}\beta\left(\frac{1}{2\tau_n}(|\omega| - \omega_n + \tau_n)\right)\right] \text{ if } \omega_n - \tau_n \le |\omega| \le \omega_n + \tau_n \quad (5)$$

$$\hat{\phi_n}(\omega) = 0 \text{ otherwise}$$

Statistical analysis

For comparing the parameters of Mean, Standard deviation and Entropy SPSS version 2.1 software is used. The independent samples T-test and group statistics are calculated using SPSS software (Gould, Dickinson, and Loftin 2018). This software is used to measure the Mean, Standard deviation, and significant difference between two groups. The simulated mean value and standard deviation are shown as graphical representation and tabulation. In this study, independent variables are the input features such as contrast, quality and edge. The dependent variables are mean, standard deviation and entropy are the output parameters (Shrestha et al. 2011).

V. RESULTS

This study observes that the Entropy is improved in percentage by using different samples and by using different algorithms. Entropy is measured for 20 sample images taken in Table 1. These were simulated in the SPSS software for means of comparison between EWT and NNF Algorithm and get the group statistics for the algorithm which contains the mean values of the Entropy and standard deviation has been given in Table 2 which is taken from SPSS outputs. Table 3 shows the testing of independent variables in which significance has been given for the EWT and NNF Algorithm and in the table mean difference and standard error difference.

Simulation block diagram of Conjunctiva of eye color change using microscope images through EWT is shown in fig. 1. Bottom to Top eye image was captured using a thermal camera shown in fig. 2. Right to Left eye image of the microscope was captured using a thermal camera. are shown in fig. 3. Right to Left sub band images of the eye from EWT2D are shown in fig. 4. Bottom to Top sub band images of the eye from EWT2 are shown in fig. 5. Statistical analysis of Conjunctiva of eye color change using microscope images through thermal image and comparison of EWT and DWT techniques in terms of tortuosity is shown in fig. 6.

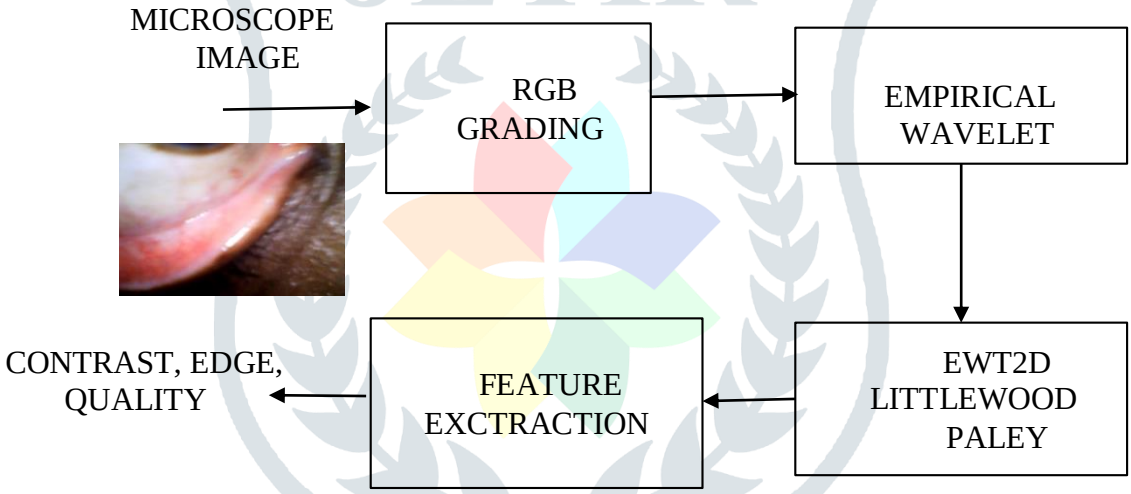

Fig. 1. Simulation block diagram of Conjunctiva of Eye Colour Change Assessment Using Microscope Image for Improving Tortuosity Through EWT.

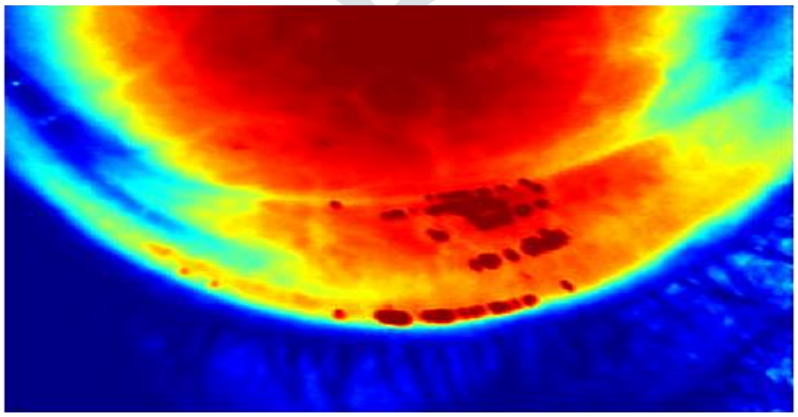

Fig. 2. Bottom to Top eye image was captured using a thermal camera.

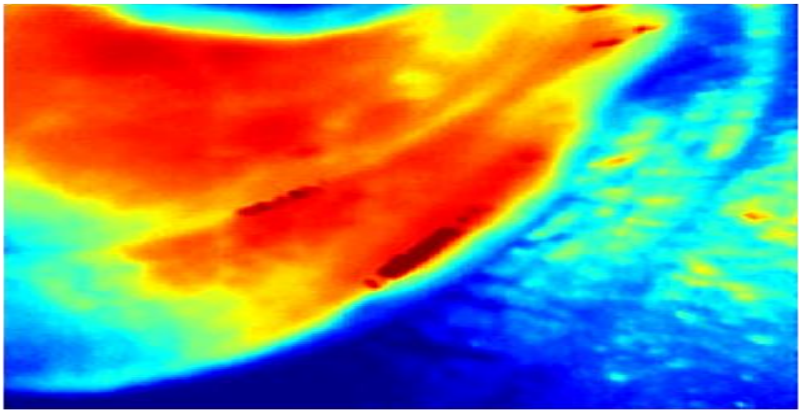

Fig. 3. Right to Left eye image of the microscope was captured using a thermal camera.

Fig. 4. Right to Left subband images of eye from EWT2D

Fig. 5. Bottom to Top subband images of eye from EWT2D

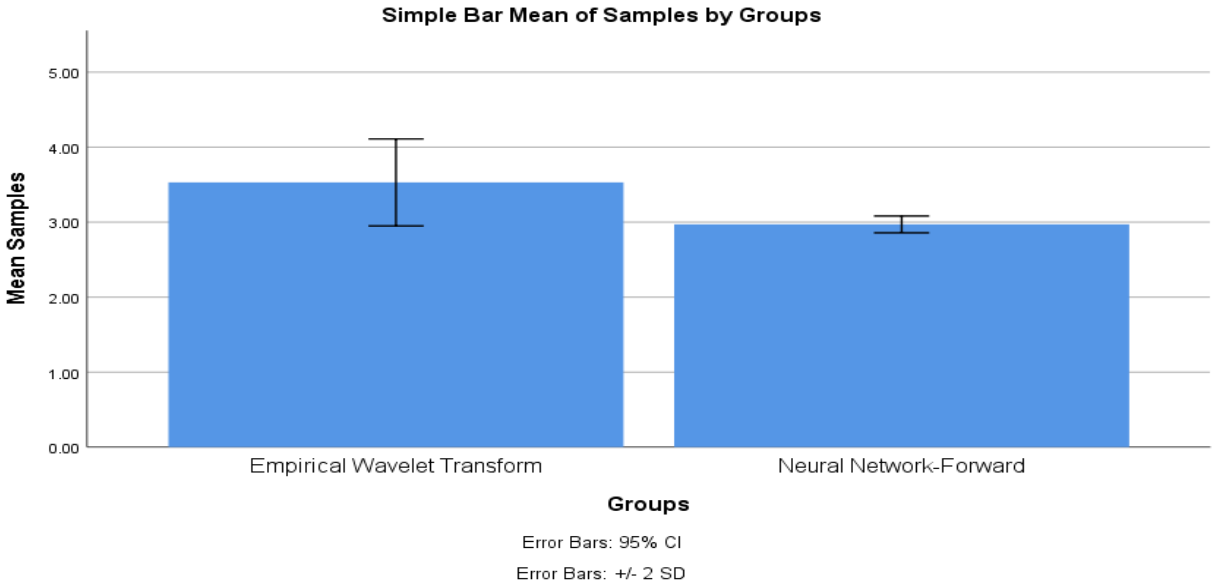

Fig. 6. Statistical analysis of conjunctiva using thermal images through the thermal image.Comparison of EWT and NNF techniques in terms of SSIM. The mean tortuosity is better than NNF and the standard deviation of EWT is slightly better than NNF. X Axis: EWTvs NNF Y Axis: Mean tortuosity of detection ± 1 SD.

Table 1. shows the percentage of Entropy acquired between the EWT and NNF Algorithm.

Samples	Entropy	
	EWT	NNF
1	3.1273	2.9116
2	3.1978	2.9263
3	3.2968	2.9336
4	3.3692	2.9416
5	3.4562	2.9556
6	3.5678	2.9654
7	3.6514	2.9765
8	3.7892	2.9882
9	3.8672	2.9968
10	3.9778	3.1095

Table 2. Group Statistics Results-EWT has a mean accuracy (3.5301), std.deviation (.28979), whereas Neural Network has mean accuracy (2.9702), std.deviation (.05591).

Group Statistics					
Tortuosity	Group	N	Mean	Std.Deviation	Std.Error Mean
	EWT	10	3.5301	.28979	.09164
	NN	10	2.9702	.05591	.01768

Table 3. Independent Samples T-test - EWT seems to be significantly better than Neural Networks (sig = .001)

	Tortuosity	Independent Samples Test								
		Levene's Test for Equality of Variances		T-test for Equality of Means						
		F	Sig	t	df	Sig(2-tailed)	Mean Difference	Std.Error Difference	95% Confidence Interval of the Difference	
									Lower	Upper
Values	Equal variances assumed	19.454	.001	5.999	18	.000	.55986	.09333	.36378	.75594
	Equal variances not assumed			5.999	9.669	.000	.55986	.09333	.35094	.76878

VI.DISCUSSION

In this study we observed the EWT as a tortuosity value and entropy when compared to the Neural Network Forward algorithm by performing an independent t-test. and mean 87.5 % the proposed algorithm reduces the loss percentage in the value and improves the mean. The total value is found to be < 0.0005. This shows that the study has met 95 % respectively.

Palpebral conjunctival hyperemia may be redder than predicted this is most likely due to typical physiological detail observable by slit-lamp microscopy, rather than a fault in the grading scale's design, the results of the second test increase by 20.9 % after using this approach of automated segmentation of the palpebral conjunctiva (Delgado-Rivera et al. 2018). When the blood vessels of the bulbar conjunctiva get clogged, a distinctive red color develops in the region. The average variance for the right eye is 0.19286, and for the left eye is 0.15714, using a completely automated system for hyperemia grading in the bulbar conjunctiva. Fifty percent of the photographs have the same assessment (Brea et al. 2017). The conjunctival microcirculation is accessible for direct inspection and quantitative measurement of microvascular hemodynamic characteristics. Conjunctival V was lower in venules than in arterioles, although the difference was modest (P = 0.05). Conjunctival WSR was substantially lower in venules than in arterioles (P = 0.001) (Khansari et al. 2016). They present a non-invasive technique to Hb estimate based on image analysis of a specific conjunctival area utilizing the k-nearest neighbor classification algorithm for assessing the (non)anemic status, which provides satisfactory results and allows clinicians to save a large number of blood tests, they rate the patient's condition as high-risk (Hb 10.5 g/dl), uncertain (10.5 Hb 11.5), and low-risk (Hb > 11.5) (Dimauro, Caivano, and Girardi 2018). The analysis of Conjunctival impression cytology (CIC) allows for the sample of cells from the bulbar conjunctiva without the requirement for surgical intervention in order to examine the overall health of the conjunctival surface. These varied from 11.5 percent to 81.4 percent of the group mean values, with an overall mean of 43.8 percent (Doughty 2010).

The upper tarsal conjunctiva is constantly in touch with the surface of the contact lens and an analysis revealed that 75 % of the patients were between the ages of 20 and 30 and female contact lens wearers outweighed male contact lens wearers by a 9:1 ratio.(Anshu et al. 2001). This work presents two image processing and machine learning-based approaches for assessing conjunctival vasculature using ordinary digital pictures. The correlation coefficient for the entire dataset (training and validation) for the Artificial Neural Networks (ANN) technique is 0.8723 (Derakhshani, Saripalle, and Doynov 2012).

VII. CONCLUSION

It is observed that EWT has a higher average tortuosity of 3.7892 than DWT with an average tortuosity of 3.1095. In this study of improved tortuosity in the Conjunctiva of eye color change assessment using microscope images, the EWT that operates using Matlab software appeared to give better results when compared to DWT. The performance also continuously increased with an increase in data which is not seen in other algorithms. This model is very efficient and holds a good potential to improve Innovative conjunctiva of eye color change assessment, hence can be implemented. EWT has a greater average tortuosity of 3.7892 than DWT, which has a tortuosity of 3.1095. When compared to the DWT in this investigation of enhanced tortuosity in the Conjunctiva of eye color change evaluation utilizing microscope images, the EWT that works using Matlab software seems to produce superior findings. The performance of the algorithm also grew continually as the amount of data increased, which is not

seen in other methods. This model is extremely efficient and has a high potential for improving Innovative conjunctiva of eye color change evaluation, therefore it may be used.

REFERENCES

[1] Anshu, M. M. Munshi, V. Sathe, and A. Ganar. 2001. "Conjunctival Impression Cytology in Contact Lens Wearers." *Cytopathology: Official Journal of the British Society for Clinical Cytology* 12 (5): 314–20.

[2] Brea, Luisa Sanchez, Noelia Barreira Rodriguez, Antonio Mosquera Gonzalez, and Katharine Evans. 2017. "Assessment of the Repeatability in an Automatic Methodology for Hyperemia Grading in the Bulbar Conjunctiva." *2017 International Joint Conference on Neural Networks (IJCNN)*. https://doi.org/10.1109/ijcnn.2017.7966052.

[3] Chen, Yihui, Xiaoyan Zhang, Ling Yang, Min Li, Bing Li, Weifang Wang, and Minjie Sheng. 2014. "Decreased PPAR-γ Expression in the Conjunctiva and Increased Expression of TNF-α and IL-1β in the Conjunctiva and Tear Fluid of Dry Eye Mice." *Molecular Medicine Reports* 9 (5): 2015–23.

[4] Delgado-Rivera, Gerson, Avid Roman-Gonzalez, Alicia Alva-Mantari, Bryan Saldivar-Espinoza, Mirko Zimic, Franklin Barrientos-Porras, and Mario Salguedo-Bohorquez. 2018. "Method for the Automatic Segmentation of the Palpebral Conjunctiva Using Image Processing." *2018 IEEE International Conference on Automation/XXIII Congress of the Chilean Association of Automatic Control (ICA-ACCA)*. https://doi.org/10.1109/ica-acca.2018.8609744.

[5] Derakhshani, Reza, Sashi K. Saripalle, and Plamen Doynov. 2012. "Computational Methods for Objective Assessment of Conjunctival Vascularity." *Conference Proceedings: ... Annual International Conference of the IEEE Engineering in Medicine and Biology Society. IEEE Engineering in Medicine and Biology Society. Conference* 2012: 1490–93.

[6] Dimauro, Giovanni, Danilo Caivano, and Francesco Girardi. 2018. "A New Method and a Non-Invasive Device to Estimate Anemia Based on Digital Images of the Conjunctiva." *IEEE Access*. https://doi.org/10.1109/access.2018.2867110.

[7] Doughty, M. J. 2010. "Assessment of Agreement for Assignment of a Normal Grade to Human Conjunctival Impression Cytology Samples." *Cytopathology*. https://doi.org/10.1111/j.1365-2303.2009.00728.x.

[8] Fielding, Henry. 2008. "Containing a Scene of Distress, Which Will Appear Very Extraordinary to Most of Our Readers." *Tom Jones*. https://doi.org/10.1093/owc/9780199536993.003.0167.

[9] Ganesh, Tameshwar, Marvin Estrada, Herman Yeger, James Duffin, and Hai-Ling Margaret Cheng. 2017. "A Non-Invasive Magnetic Resonance Imaging Approach for Assessment of Real-Time Microcirculation Dynamics." *Scientific Reports*. https://doi.org/10.1038/s41598-017-06983-6.

[10] Gould, Paul, Travis Dickinson, and Keith Loftin. 2018. *Stand Firm: Apologetics and the Brilliance of the Gospel*. B&H Academic.

[11] Huang, Norden E., Zheng Shen, Steven R. Long, Manli C. Wu, Hsing H. Shih, Quanan Zheng, Nai-Chyuan Yen, Chi Chao Tung, and Henry H. Liu. 1998. "The Empirical Mode Decomposition and the Hilbert Spectrum for Nonlinear and Non-Stationary Time Series Analysis." *Proceedings of the Royal Society of London. Series A: Mathematical, Physical and Engineering Sciences*. https://doi.org/10.1098/rspa.1998.0193.

[12] Iroshan, K. A., A. D. N. De Zoysa, C. L. Warnapura, M. A. Wijesuriya, S. Jayasinghe, N. D. Nanayakkara, and A. C. De Silval. 2018. "Detection of Diabetes by Macrovascular Tortuosity of Superior Bulbar Conjunctiva." *Conference Proceedings: ... Annual International Conference of the IEEE Engineering in Medicine and Biology Society. IEEE Engineering in Medicine and Biology Society. Conference* 2018 (July): 1–4.

[13] Katzir, Gadi, and Graham R. Martin. 2008. "Visual Fields in the Black-Crowned Night Heron Nycticorax Nycticorax: Nocturnality Does Not Result in Owl-like Features." *Ibis*. https://doi.org/10.1111/j.1474-919x.1998.tb04554.x.

[14] Khansari, Maziyar M., Justin Wanek, Anthony E. Felder, Nicole Camardo, and Mahnaz Shahidi. 2016. "Automated Assessment of Hemodynamics in the Conjunctival Microvasculature Network." *IEEE Transactions on Medical Imaging* 35 (2): 605–11.

[15] McCormick, Keith, and Jesus Salcedo. 2017. *SPSS Statistics for Data Analysis and Visualization*. John Wiley & Sons.

[16] Shrestha, E., J. K. Shrestha, G. Shayami, and M. Chaudhary. 2011. "The Conjunctival Impression Cytology between the Diagnosed Cases of Dry Eye and Normal Individuals." *Nepalese Journal of Ophthalmology: A Biannual Peer-Reviewed Academic Journal of the Nepal Ophthalmic Society: NEPJOPH* 3 (1): 39–44.

[17] Tamir, Azwad, Chowdhury S. Jahan, Mohammad S. Saif, Sums U. Zaman, Md Mazharul Islam, Asir Intisar Khan, Shaikh Anowarul Fattah, and Celia Shahnaz. 2017. "Detection of Anemia from Image of the Anterior Conjunctiva of the Eye by Image Processing and Thresholding." *2017 IEEE Region 10 Humanitarian Technology Conference (R10-HTC)*. https://doi.org/10.1109/r10-htc.2017.8289053.